Journal of Sciences, Islamic Republic of Iran 24(2): 129-134 (2013) http://jsciences.ut.ac.ir
University of Tehran, ISSN 1016-1104

Thermal Behavior of a Natural Sepiolite from Northeastern Iran

S. Hojati[1,*] and H. Khademi[2]

[1]*Department of Soil Science, College of Agriculture, Shahid Chamran University, Ahvaz 6135783151, Khuzestan, Islamic Republic of Iran*
[2]*Department of Soil Science, College of Agriculture, Isfahan University of Technology, Isfahan 8415683111, Isfahan, Islamic Republic of Iran*

Received: 19 August 2012 / Revised: 6 February2013 / Accepted: 14 May 2013

Abstract

Sepiolite deposits have been recently discovered in northeastern Iran. However, there is still little information about its physicochemical and mineralogical characteristics. Therefore, the collapse of the sepiolite (with sizes of < 63 μm) structure induced by temperature elevation in an electric furnace at 350, 550, and 850 °C for 4 hours was studied using X-ray diffraction (XRD) in combination with Thermogravimetric analysis (TGA) and infrared spectroscopic analysis. Results showed that the main mineral constituent of the samples is a well crystallized sepiolite. However, dolomite and quartz were also present in minor amounts. Results also revealed that with temperature different phases including 'sepiolite dihydrite', 'sepiolite anhydrite' and 'enstatite' were formed, as magnesium coordinated water and octahedrically coordinated hydroxyl groups, were eliminated and the dehydroxylated phase was recrystallized to enstatite, a stable form of magnesium silicate ($MgSiO_3$).

Keywords: Sepiolite; Enstatite; Zeolitic water; Infrared spectroscopy

Introduction

Sepiolite belongs to the phyllosilicate group of 2:1 clay minerals which is widely distributed in soils and sediments of arid and semi-arid regions [22]. The modular structure of sepiolite is composed of alternating talc-like ribbons and tunnels, extended along the z-direction of the crystal [23]. The tetrahedral sheet is continuous across the ribbons but periodic inversion of the octahedral sheet makes it discontinuous; thus, terminal octahedral cations must complete their coordination sphere with water molecules called as coordinated water [10].

The idealized formula of sepiolite is $Mg_8Si_{12}O_{30}(OH)_4(OH_2)_4 \cdot xH_2O$ (x = 6-8), where (OH_2) group denotes crystal water and H_2O as zeolitic water [18]. Since the sepiolite ribbons are held together by Si-O-Si bindings, the change of interlayer spacing caused by H_2O content variation is constrained. Therefore, dehydration process imposes structural rearrangements within the corresponding layer [11].

Structural and morphological characteristics of sepiolite cause specific physicochemical properties such as high porosity and surface area, strong adsorptive

* Corresponding author, Tel.: +98(611)3364054, Fax: +98(611)3330079, E-mail: s.hojati@scu.ac.ir

power, and high capacity to hold heavy metals. These properties give sepiolite a broad range of applications such as in molecular sieving, decolorization, oil refining, pesticide carrier, and wastewater treatment technology [18, 16]. Thermal treatment of sepiolite is a necessary process for almost all of its applications, especially in rubber industry [2, 3]. Some of thermoanalytical methods such as Differential Thermal Analysis (DTA) and Thermogravimetric Analysis (TGA) can provide a measure of the thermal stability for some clay minerals including sepiolite [8]. These techniques in combination with X-ray diffraction (XRD) and Fourier transform infrared spectroscopy (FTIR) have proved to be useful for the study of the dehydration and dehydroxylation processes induced by heat treatment in clay minerals [2, 8]. Although occurrences of sepiolite have been reported in USA, Kenya, Spain, Portugal, Turkey, Saudi Arabia, Great Britain, and Morocco [16], no reports have been yet documented regarding the existence of this mineral in Iran. Deposits of sepiolite have been recently found in northeastern Iran and mining of them have already been started. However, there is still little information about physicochemical and mineralogical characteristics of these deposits [13]. Besides, natural samples from mines usually contain non-clay minerals such as carbonates and dolomites; and therefore, it is very interesting to study the thermal behavior of such a sample. The present study aims to investigate the collapse of the sepiolite structure induced by temperature elevation as revealed by X-ray diffraction (XRD) in combination with Thermogravimetric analysis (TGA) and infrared spectroscopic analysis.

Materials and Methods

Sample Preparation

Sepiolite samples were taken from Fariman deposits in northeastern Iran. Initially, the samples were sieved to the sizes of < 63 μm. Chemical composition of the sepiolite sample is shown in Table 1. The samples were calcined in an electric furnace at 350, 550, and 850 °C for 4 hours, cooled down in desiccators, and immediately used for further analyses.

X-ray Diffraction

The XRD patterns of the samples (powdered and calcined sepiolites) were performed with a Philips diffractometer (PW1840) apparatus with Cu-Kα radiation at ambient temperature (25°C). The scanning was performed in step-scan mode over the 2θ range 2-40° with a step size of 0.02° and counting time of 0.5 s per step. Diffraction patterns were recorded at 40kV and 30mA.

Thermogravimetric Analysis

Thermal characterization of the samples was performed on an approximately 100 mg samples using a Bahr STA Type 503 instrument under 100 ml min^{-1} nitrogen /air flow. Each sample underwent the thermal analysis in the temperature range of 35-1100 °C and a heating rate of 10 °C min^{-1}.

Infrared Spectroscopy

Samples were prepared with mixing each powdered sample with oven-dried KBr at 105°C (the blank) in an 1:200 ratio and FTIR spectra for the studied samples were determined with a spectral resolution of 8 cm^{-1} over the wavenumber range of 400-4000 cm^{-1} on a Bruker Tensor 27 FTIR spectrophotometer.

Results and Discusion

X-ray Diffraction

Results of XRD pattern analysis of the raw and thermally treated sepiolite samples are shown in Fig. 1. Results imply that the raw material is a highly crystalline solid, as confirmed by the presence of a sharp and strong diffraction peak at d_{110} = 1.206 nm (Fig. 1). Results also indicate that the studied sepiolite samples contain minor amounts of dolomite (d_{104} = 0.286 nm) and quartz (d_{101} = 0.334 nm) as accompanying phases [13]. Other peaks detected in the pattern belong to the sepiolite [5, 19, 21, 22].

The XRD pattern analysis of heat treated samples revealed that the heating caused structural and textural changes associated with the dehydration and dehydroxylation processes (Fig. 1). Calcination at 350°C caused a slight decrease in line intensity of sepiolite (1.206 nm) and created new peaks at 1.018 and 0.813 nm. Similar results were also reported by Perraki and Orphanoudaki [18]. They attributed the presence of these peaks to the formation of the new phase of "sepiolite dehydrate" that can be expressed by the following reaction:

$$Mg_8Si_{12}O_{30}(OH)_4.(H_2O)_4.nH_2O \rightarrow Mg_8Si_{12}O_{30}(OH)_4.(H_2O)_2 + 2H_2O \quad (1)$$

In this temperature the surface water and water bonded to exchangeable cations in the raw material

were removed, but crystal structure of sepiolite was maintained (Fig. 1). Heatng the samples up to 550°C, totally eliminated the peak at 12.06 nm, indicating the total degradation of sepiolite dihydrite. The slight increase in the peaks at ~1.018 and ~0.813 nm (Fig. 1) indicates the formation of sepiolite anhydrite based on the below reaction:

$$Mg_8Si_{12}O_{30}(OH)_4.(H_2O)_2 \rightarrow$$

$$Mg_8Si_{12}O_{30}(OH)_4. + 2H_2O \quad (2)$$

After heating of the sample up to 850°C (Fig. 1), peaks at ~1.0 and ~0.8 nm were also disappeared, and new peaks at 0.288, 0.318 and 0.254 nm appeared suggesting the formation of enstatite (MgSiO3) [4, 18].

Thermogravimetric Analysis

Four mass losses were observed at 127, 343, 464 and 818 °C accompanying by mass loss percentages of 8.69, 3.3, 2.65, and 10.19, respectively (Fig. 2). These steps correspond to (a) the loss of adsorbed water, (b) the loss of hydration water, (c) the loss of coordination water, and (d) the loss of water through dehydroxylation, respectively [4]. The following Eqs. represent these schemes:

$$Mg_8Si_{12}O_{30}(OH)_4.(H_2O)_4.8H_2O \longrightarrow$$

$$Mg_8Si_{12}O_{30}(OH)_4.(H_2O)_4 + 8H_2O \quad (3)$$

$$Mg_8Si_{12}O_{30}(OH)_4.(H_2O)_4 \longrightarrow$$

$$Mg_8Si_{12}O_{30}(OH)_4.(H_2O)_2 + 2H_2O \quad (4)$$

$$Mg_8Si_{12}O_{30}(OH)_4.(H_2O)_2 \longrightarrow$$

$$Mg_8Si_{12}O_{30}(OH)_4 + 2H_2O \quad (5)$$

$$Mg_8Si_{12}O_{30}(OH)_4 \longrightarrow$$

$$8MgSiO_3 + 4SiO_2 + 2H_2O \quad (6)$$

If the formula $(Mg_8Si_{12}O_{30}(OH)_4.(H_2O)_4.8H_2O)$ is taken into account for chemical composition of sepiolite, then the theoretical mass losses for steps 1 to 4 should be 11.0, 3.3, 2.8, and 2.8% [17]. In the first step, the assessments on the sepiolite samples showed an 8.69% (11.0% calculated value) mass loss because of the removal of zeolitic or channel water. The difference between the measured and calculated values is probably related to the evolving some loosely bound zeolitic water from sepiolite samples during time required for the initial conditioning at 35°C prior to the programmed heating. The loss of this hydration water was completed at 127°C and followed by two other steps of

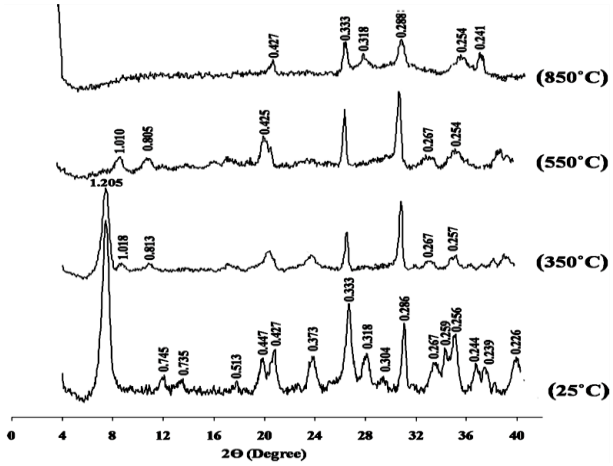

Figure 1. XRD pattern analysis of the natural and thermally treated sepiolite samples.

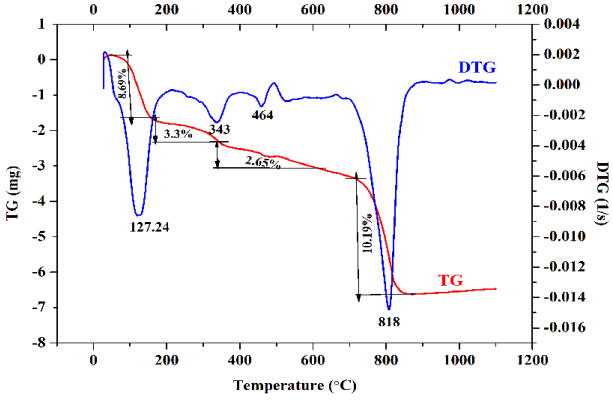

Figure 2. TG and DTA curves of the natural sepiolite sample in the temperature range of 35-1100 °C showing four distinct mass losses at 127, 343, 464 and 818 °C.

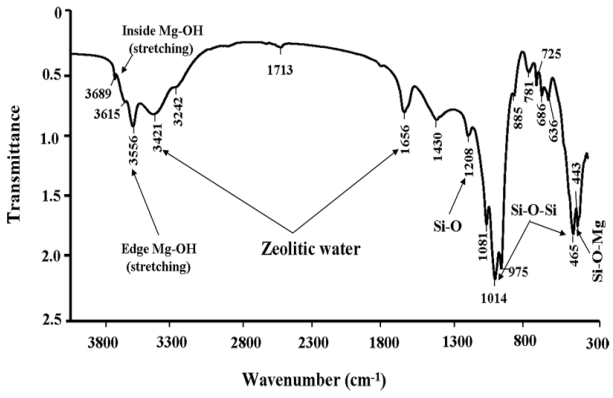

Figure 3. Fourier transform infrared spectroscopy analysis of sepiolite samples showing signals for different types of water and hydroxyl groups at the mineral surface.

dehydration in which sepiolite lost the coordinated water. Half of the coordinated water was lost in the second dehydration process at 343 °C with a 3.3% mass loss (3.3% calculated value) while the last part was lost at higher temperatures 464 °C with a further equivalent mass loss (2.65%). With increasing the temperature to 818 °C another degradation step which caused a 10.19% mass loss occured because of the dehydroxylation of sepiolite anhydrite that losses its structure [14, 17, 19], the degradation of dolomite to calcite at 600 °C, and the degradation of calcite at temperatures between 740 to 850 °C [20]. This step, which results in the formation of enstatite and silica, was completed at 818 °C.

Infrared Spectroscopy

The FTIR analysis of the sepiolite and its calcination products are presented in Fig. 3 and Table 2. Based on that, three distinct wavenumber regions including 4000 to 2800 cm^{-1}, 1800 to 1400 cm^{-1}, and 1400 to 400 cm^{-1} are observed (Fig. 3). The zone in the range from 4000 to 2800 cm^{-1} show bands corresponding to the vibrations of different types of hydroxyl groups [2, 7, 9, 12, 15]. The zone from 1800 to 1400 cm^{-1} range is very asymmetric and contained OH bond deformation bands. Based on Frost et al. [7], asymmetry in this zone can be attributed to the presence of different types of water molecules. Previous absorption studies have shown the existence of two partially resolved peaks at 1630 and 1656 cm^{-1} which were attributed to the adsorbed and zeolitic water [6].The zone from 1400 to 400 cm^{-1} corresponds mainly to the band characteristics of silicate minerals, typical stretching vibrations of Si–O bonds and the deformation vibrations of O–H bonds [15, 18].

Although some previous studies showed a band at 3720 cm^{-1} that was attributed to OH stretching vibrations in silanol groups (Si–OH) [7], the spectrum obtained from the Fariman sepiolite showed no band at this region suggesting low amounts of silanol groups in the mineral structure. Another possibility is the reaction of silanol groups with the KBr. More studies are needed to verify this hypothesis. The band observed at 3615cm^{-1} can be attributed to the stretching modes of hydroxyl groups coordinated with the magnesium [2, 3]. According to Chahi et al. [1] and Frost et al. [9], the band at 3556 cm^{-1} can be also attributed to the stretching vibration of Al–Fe^{3+}–OH or Al–Mg–OH band. The difference in the bands position in this study and previous ones may arise from the variations in the mineral composition, sample origin and impurities. Further studies are needed to shed light on this matter.

Results revealed that the spectra for the raw sepiolite and its calcination product at 350°C (Table 2) contained the same bands but with lower intensity for the absorption bands at 3569, 3421 and 1651 cm^{-1} in the calcined product (Table 2). These bands are firstly lost during calcination as a result of the gradual dehydration and dehydroxylation of the thermally treated sepiolite samples with no significant effect on the sepiolite structure. These results are consistent with the XRD patterns, which showed no significant changes in the diffraction bands after calcination at 350 °C. However, bands at ~1019 and ~465 cm^{-1} (because of Si–O–Si vibrations), and the band at ~443 cm^{-1}(due to Si–O–Mg), as well as those of octahedrally coordinated OH groups at ~782 and ~636 cm^{-1} remained constant during the calcination process at 350 °C. The FTIR spectra for the raw and the thermally treated samples exhibited three bands at 1210, 1076 and 1014 cm^{-1} which were assigned to the stretching vibrations of Si–O bonds. The band appeared at 1210 $cm^{-1}$is a band characteristic of minerals with tetrahedral sheet inversion (e.g. sepiolite and palygorskite) and is ascribed to Si-O-Si bond in the minerals [18]. These bands (1210, 1076 and 1014 cm^{-1}) are also followed by other four bands at ~975, ~881, ~781 and ~686 cm^{-1} because of the deformation vibrations of different types of OH groups in the solids. Our results are in agreement with those reported by Mora et al., [15] and Perraki and Orphanodaki [18].

However, calcination at 550 °C decreased the signal intensity at 3676 cm^{-1} indicating that the sepiolite structure was folded and an anhydrous form of sepiolite born [21]. As can be seen, at calcination temperature 550 °C, the signal at 3685 cm^{-1}, due to OH groups bonded to Mg in octahedral layers, was removed, and a new signal attributed to the formation of anhydrous sepiolite appeared at 3606 cm^{-1} (Table 2). Similar results were also reported by Mora et al., [15] and Frost et al., [9, 12].

Finally, calcination at 850 °C caused the removal of all hydroxyl groups as compared with the raw material. The spectrum of the calcined solid contained none of the bands induced by OH stretching vibrations in zeolitic water or magnesium coordinated water in octahedral layers. This suggests that the layered structure of sepiolite collapsed and the new phase "enstatite" formed. This is in agreement with the results obtained from XRD analysis of the samples (Fig. 1). Raising the temperature up to 850 °C resulted in the formation of enstatite as a new phase that consequently reduced the number of bands for Si–O stretching vibrations [15]. The sample calcined at 850 °C exhibited a single, broad, weak band centered at 1622 cm^{-1} which should encompass OH bending vibrations in Mg–OH groups and enstatite water [15].

Table 1. Chemical composition of the sepiolite sample used in this study [13]

Oxides	Value (g Kg^{-1})
SiO_2	553.2
Al_2O_3	3.0
Fe_2O_3	6.1
MgO	167.3
CaO	17.4
TiO_2	0.20
Na_2O	0.2
K_2O	0.1
LOI*	251.1
Total	998.6

* LOI = Loss-on-Ignition

Table 2. Changes in the infrared absorption bands of the natural sepiolite following thermal treatment

Natural	350°C	550°C	850°C	Suggested assignments
3689 w	3676 m	3674 s		Mg_3OH octahedral stretch
3615 m	3597 m	3581w		Mg_3OH octahedral stretch
3556 m	3527 m			OH-stretch from coordinated water
3421 s	3417 s	3417 s	3425 s	Water OH-stretch
3242 w	3242 w			Water OH-stretch
1713 s	1711 m	1708 w		Water OH bend
	1687		1691 w	Water OH bend
1656	1647	1624 m	1622 s	Water OH bend
1430 s	1429 s	1425 s	1400 s	Impurities of carbonates
1208 m	1201 w			Si-O stretch
1081 m	1072 w	1072 m	1068 m	Si-O stretch
1014 m	1014 w	1012 m	1004 w	Si-O stretch
975 m			925 m	OH deformation
885 w	881 w	865 m	852 w	OH deformation
781 m	790 w	796 m	792 w	OH deformation
725 m		721 m	721 s	OH deformation
	765 w	746		OH deformation
686 m	686 s	684 m	684 w	OH translation
		659 w		OH translation
636 m	644 m	632 w	638 w	OH translation
465 m	464 w	457 w	459 m	O-Si-O bends
443 m	429 w			O-Si-O bends

m= moderate; w = weak; and s= strong

Acknowledgements

The authors gratefully acknowledge Shahid Chmran University of Ahvaz and Isfahan University of Technology for the financial supports they provided for this study.

References

1. Chahi, A., Petit, S. and Decarreau, A. Infrared evidence of dioctahedral-trioctahedral site occupancy in palygorskite, *Clays Clay Miner*. **50**: 306-313 (2002).
2. Cheng, H., Yang, J. and Frost, R. L. Thermogravimetric analysis-mass spectrometry (TG-MS) of selected Chinese palygorskites-Implications for structural water, *Thermochim Acta*. **512**: 202-207 (2011).
3. Cheng, H., Yang, J., Frost, R. L. and Wu, Z. Infrared transmission and emission spectroscopic study of selected Chinese palygorskites, *Spectrochim Acta Part A.*, **83**: 518-524 (2011).
4. d'Azevedo, C.A., Garrido, F. M. S. and Medeiros, M. E. The effects of mechanochemical activation of on the reactivity in the MgO-Al2O3-SiO2 system, *J. Therm. Anal. Calor*. **83**: 649-655 (2006).
5. Erdogan-Alver, E., Sakici, M., Yorukogullari, E., Yilmaz, Y. and Guven, M. Thermal behavior and water adsorption of natural and modified sepiolite having dolomite from Turkey, *J. Therm. Anal. Calor*. **94**: 835-840 (2008).
6. Farmer, V. C. The layer silicates. In: Farmer, V.V. (Ed.), *Infrared Spectra of Minerals*, Mineralogical Society, London, pp. 331–363 (1974).
7. Frost, R.L., Cash, G.A. and Kloprogge, J. T. Rocky Mountain leather, sepiolite and attapulgite-an infrared emission spectroscopic study. *Vib Spectrosc*. **16**: 173-184 (1998).
8. Frost, R. L., Kristof, J. and Horvath, E. Controlled rate thermal analysis of sepiolite, *J. Therm. Anal. Calor*. **98**: 423-428 (2009).
9. Frost, R.L., Locos, O.B., Ruan, H. and Kloprogge, J. T. Near-infrared and mid-infrared spectroscopic study of sepiolites and palygorskites, *Vib Spectrosc*. **27**: 1-13 (2001).
10. Garcia-Romero, E. and Suarez, M. On the chemical composition of sepiolite and palygorskite, *Clays. Clay Miner*. **58**: 1-20 (2010).
11. Gionis, V. , Kacandes, G. H. and Chryssikos, G. D. Synchronous near- and mid infrared investigation of the dehydration of sepiolite. Pcoc Trilateral Meeting on Clays, Seville, Spain, 54-55 (2010).
12. Hayashi, H., Otsuka, R. and Imai, N. IR study of sepiolite and palygorskite on heating, *Am Mineral*. **53**: 1613-1624 (1969).
13. Hojati, S. and Khademi, H. Physicochemical and mineralogical characteristics of sepiolite deposits of northeastern Iran, *Ulum-e-Zamin*. In Press.
14. Lapides, I. and Yariv, S. The effects of mechanochemical treatments of sepiolite with CsClon the calcinations products, *J. Therm. Anal. Calor*. **99**: 855-860 (2010).

15. Mora, M., Lopez, I., Carmona, M. A., Jimenez-Sanchidrian, C. and Ruiz, J. R. Study of the thermal decomposition of a sepiolite by mid- and near-infrared specrtoscopies, *Polyhedron*. **29**: 3046-3051 (2010).
16. Murray, H.H. *Applied Clay Mineralogy: Occurrences, Properties and Applications of Kaolins, Bentonites, Palygorskite-Sepiolite, and Common Clays*, Elsevier, Amesterdam, (2007).
17. Nagata, H., Shimoda, S. and Sudo, T. On dehydration of bound water of sepiolite, *Clays Clay Miner*. **22**: 285-293 (1974).
18. Perraki, T., and Orfanoudaki, A. Study of raw and thermally treated sepiolite from the Mantoudi area, Euboea, Greece, *J. Therm. Anal. Calor*. **91**: 589-593 (2008).
19. Post, J.E., Bish, D.L. and Heaney, P. J. Synchrotron powder X-ray diffraction study of the structure and dehydration behavior of sepiolite, *Am. Mineral*. **92**: 91–97 (2007).
20. Rat'ko, A.I., Ivanets, A.I., Kulak, A.I., Morozov, E. A. and Sakhar, I. O. Thermal decomposition of natural dolomite, *Inorg Mater*. **47**: 1372-1377 (2011).
21. Serna, C., Ahlrichs, J. L. and Serratosa, J. M. Folding in sepiolite crystals, *Clays Clay Miner*. **23**: 452-457 (1975).
22. Singer, A. Palygorskite and sepiolite group minerals. In: Dixon, J.B. and Weed, S.B. (Eds.), *Minerals in Soil Environments*, Soil Science Society of America, Madison, pp. 829-872 (1989).
23. Yener, N., Onal, M., Ustunisik, G. and Sarikaya, Y. Thermal behavior of a mineral mixture of sepiolite and dolomite, *J. Therm. Anal. Calor*. **88**: 813-817 (2007).